American Mineralogist, Volume 84, pages 92–101, 1999

Si, Al ordering in the double-ring silicate armenite, $BaCa_2Al_6Si_9O_{30}\cdot 2H_2O$: A single-crystal X-ray and ^{29}Si MAS NMR study

THOMAS ARMBRUSTER*

Laboratorium für chemische und mineralogische Kristallographie, Universität Bern, Freiestrasse 3, CH-3012 Bern, Switzerland

ABSTRACT

The ^{29}Si MAS NMR spectrum of armenite from Wasenalp (Valais, Switzerland) indicates complete Si, Al ordering. The same chemical shifts (−82.3, −95.0, and −101.8 ppm) were also measured for armenite from Rémigny (Quebec, Canada), however, the intensity ratios of the NMR bands for the latter sample differed. A full sphere of X-ray single-crystal data on an optically homogeneous domain of armenite from Rémigny was collected on a three-circle diffractometer equipped with a CCD area-detector. The crystal structure was refined in the acentric space group *Pnc*2 [a = 18.660(2), b = 10.697(1) c = 13.874(2) Å] to R1 = 3.6% based on 4275 reflections. These results confirm complete Si, Al ordering. Mean Si-O distances range between 1.615 and 1.629 Å; mean Al-O distances between 1.734 and 1.742 Å. Calcium is sevenfold coordinated by six framework O atoms and one H_2O molecule. Barium is 12-fold coordinated by framework O atoms. Polarized IR spectra in the region of OH absorptions (between 5700 and 1300 cm^{-1}) were recorded on polished slabs of Wasenalp armenite and structurally related milarite from Val Giuf. In general, milarite and armenite show similar anisotropy of H_2O related absorptions.

INTRODUCTION

Armenite, $BaCa_2Al_6Si_9O_{30}\cdot 2H_2O$, named after its first description from the Armen mine, Kongsberg, Norway (Neumann 1941), is a rather rare silicate mineral found in Ba-rich hydrothermal veins or fissures (e.g., Pouliot et al. 1984; Mason 1987; Semenenko et al. 1987; Zak and Obst 1989; Balassone et al. 1989; Senn 1990; Fortey et al. 1991). In hitherto described occurrences armenite displays a complicated twinning pattern and has essentially end-member composition with a constant Si/Al ratio of 9/6.

Armenite possesses six-membered double-rings of tetrahedra and is a member of the milarite-group of minerals (Hawthorne et al. 1991). Among this group, armenite has the most pronounced Al ↔ Si substitution, which may be responsible for a deviation from hexagonal symmetry (Armbruster and Czank 1992) observed for most other members of this group. Previous single-crystal X-ray and TEM studies (Armbruster and Czank 1992; Ferraris et al. 1991) indicated that various armenite modifications with variable degrees of Si, Al ordering give rise to different super-structures. Recently, Winter et al. (1995) studied the hexagonal structure of the high-temperature synthetic double-ring silicate $BaMg_2Al_6Si_9O_{30}$, which has the same Al/Si ratio as armenite but Ca is replaced by Mg and the synthetic compound is anhydrous.

Milarite, a fissure mineral with the simplified formula $KNa_{1-x}Ca_2(Be_{3-x}Al_x)Si_{12}O_{30}\cdot nH_2O$, shows similar anomalous optical properties as armenite (e.g., Černý et al. 1980; Janeczek 1986), which were interpreted to be caused by long range H_2O ordering (Armbruster et al. 1989).

Two topologically distinct types of tetrahedra exist in the milarite group of minerals: tetrahedra building the double-ring units (12 T1 pfu) and the ring-connecting tetrahedra (3 T2 pfu), which alternate with edge-sharing CaO_6 octahedra to form twelve-membered rings (Fig. 1). In milarite T1 tetrahedra are occupied by Si only, whereas in armenite Si and Al share T1 sites (Armbruster and Czank 1992). The T2 tetrahedra in milarite show a mixed Al, Be occupation (e.g., Černý et al. 1980; Armbruster et al. 1989) and in armenite a mixed Si, Al occupation. O2 connects T1 to six-membered rings, O1 connects the six-membered rings to double-ring units, and O3 connects the double-ring units to T2 tetrahedra thus a tetrahedral framework is formed. Above and below the double-ring units the structural channels are plugged by Ba (armenite) or K (milarite). In armenite (Armbruster and Czank 1992) and milarite (Armbruster et al. 1989) H_2O occupies structural interstices (B′ sites) close to Ca and increases the Ca coordination from six to seven. Armenite is completely hydrated and has 2 H_2O pfu. Millarite has non-stoichiometric $H_2O \ll 2$ pfu and additional Na, K, and Ca may enter the ninefold-coordinated B site, which is 0.7 Å apart from B′.

The cordierite, $Mg_2Al_4Si_5O_{18}$, and beryl, $Al_2Be_3Si_6O_{18}$, structures are closely related to double-ring silicates (e.g., Armbruster et al. 1995). Six-membered single-rings in cordierite and beryl are also connected by additional T sites to form a framework. Unfortunately, a different no-

* E-mail: armbruster@krist.unibe.ch

0003–004X/99/0102–0092$05.00

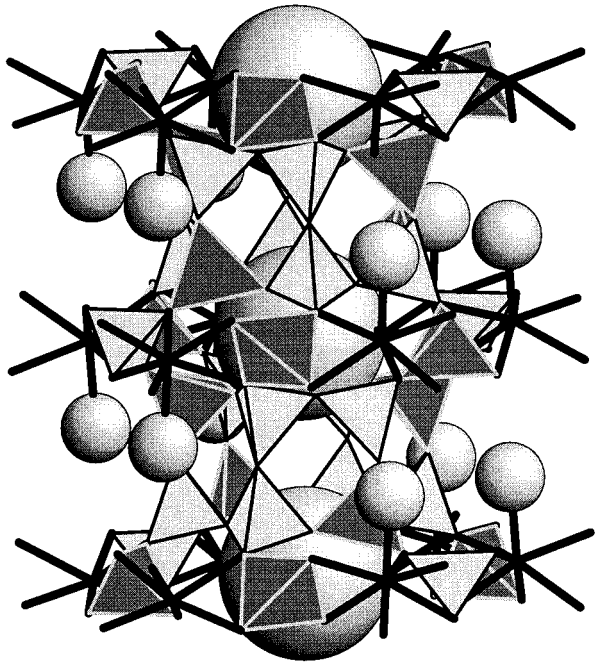

FIGURE 1. Characteristic portion of the armenite structure (space group *Pnc*2) showing the tetrahedral double-ring units projected perpendicular to the *c* axis. Light tetrahedra with dark rims are occupied by Si whereas dark tetrahedra with light rims are occupied by Al. Tetrahedra connecting double-ring units have common edges with CaO_7 polyhedra represented by thick black Ca-O bonds. The H_2O molecule bonded to Ca is shown as medium size sphere. The large sphere is Ba occupying the cage between to adjacent double-ring units. Notice the ordered arrangement of H_2O molecules either above or below the Ca polyhedron.

menclature (e.g., Cohen et al. 1977) is used for cordierite and beryl where the ring tetrahedra are named T2 and the ring connecting tetrahedra T1 (just reversed to the nomenclature of double-ring silicates). For a direct comparison between structures with single- and double-six-membered rings, a standardized labeling is introduced where T_c designates tetrahedra connecting ring units (single or double) to a tetrahedral framework. T_s are tetrahedra in single six-membered rings (beryl and cordierite) and T_d are tetrahedra assembled to six-membered double-rings (e.g., armenite and milarite).

With respect to Si, Al ordering, cordierite seems to be an analogue of armenite. In both minerals $T_{s,d}$ and T_c tetrahedra may be occupied by Si and Al in a way that Al tetrahedra are always adjacent to Si tetrahedra, in agreement with Loewenstein's (1954) rule. The Al concentration in both minerals corresponds to the maximum value allowed by this Al-avoidance rule. The two available structure refinements on optically untwinned armenites (Ferraris et al. 1991; Armbruster and Czank 1992) were performed on samples from Su Zurfuru, Sardinia, Italy (Balassone et al. 1989) and from Rémigny, Quebec, Canada (Pouliot et al. 1984). Both structures were solved in the same orthorhombic space group No. 52 (*Pnna* in standard setting) but led to different Si, Al distributions. Based on T-O distances, armenite from Su Zurfuru has the structural formula $BaCa_2[^{Tc}Al_3{}^{Td}(Al_3Si_9)O_{30}]\cdot 2H_2O$, whereas armenite from Rémigny has the formula $BaCa_2[^{Tc}(Al_2Si)^{Td}(Al_4Si_8)O_{30}]\cdot 2H_2O$. The latter formula can also be obtained by complete Si, Al ordering according to Loewenstein's (1954) rule, however, in that case the space group must be lowered to *Pnc*2 (Armbruster and Czank 1992). Armenite from Sardinia has a statistical Si, Al distribution within the T_d double-ring units leading to a Si, Al arrangement that satisfies hexagonal symmetry (Ferraris et al. 1991). The orthorhombic symmetry is caused by displacements of CaO_6 octahedra and neighboring water molecules (Ferraris et al. 1991). In the *Pnna* refinement model for the sample from Canada (Armbruster and Czank 1992) well-ordered Si, Al clusters alternate with Si, Al disordered T_c and T_d tetrahedra. The presence of both Si, Al ordered and disordered clusters within the same structure was considered highly unusual (Armbruster and Czank 1992). The question thus arouses whether the optically homogeneous crystal fragment from Rémigny was composed of completely ordered submicroscopic domains in a twin relationship or whether the strong pseudo-hexagonal symmetry led to correlation problems prohibiting a refinement of a completely Si, Al ordered model. The structure of the synthetic double-ring silicate, $BaMg_2Al_6Si_9O_{30}$, is truly hexagonal (space group *P*6/*mcc*) with a Si/Al ratio of 3/1 in the six-membered double-rings (statistically distributed) and only Al in the tetrahedra connecting the double-rings to a framework (Winter et al. 1995). Thus, Si, Al ordering in this sample is the same as in armenite from Sardinia (Ferraris et al. 1991).

A similar relationship to that between the tetrahedral frameworks of cordierite and armenite exists between beryl and milarite. In the latter pair of minerals, T_s and T_d tetrahedra are occupied by only Si whereas T_c tetrahedra are Be-rich.

One aim of the present study is to determine Si, Al ordering in armenite by ^{29}Si MAS NMR spectroscopy. This technique is powerful in distinguishing SiO_4 clusters with chemically different adjacent tetrahedra. In previous ^{29}Si MAS NMR studies on Si, Al-ordering in cordierite (Putnis et al. 1985; Hölscher and Schreyer 1989; Senegas et al. 1991) T_s(Si) tetrahedra with 1, 2, 3, and 4 adjoining AlO_4 tetrahedra could be resolved leading to four different ^{29}Si NMR chemical shifts. In addition T_s tetrahedra could be distinguished from T_c tetrahedra.

If we assume complete Si, Al ordering in armenite according to Loewenstein's (1954) rule, four T_d(Si) tetrahedra pfu corner-linked with two AlO_4 and two SiO_4 tetrahedra (2Al,2Si) and additional four T_d(Si) tetrahedra pfu corner-linked with three AlO_4 and one SiO_4 tetrahedra (3Al,1Si) should be resolved. In addition, one T_c(Si) tetrahedron is surrounded by four AlO_4 tetrahedra (4Al). Milarite has 12 T_d(Si) tetrahedra connected to either (1Be,3Si) or (1Al,3Si). For a better assignment of the chemical shifts in the armenite ^{29}Si MAS NMR spectra

and for comparison with beryl and cordierite literature data, additional spectra of milarite are needed.

Furthermore, the development of a new generation of X-ray detectors based on the CCD chip enables fast collection of precise single-crystal data. A rough estimate indicates that for a successful refinement of armenite in space group *Pnc*2 a full sphere of diffraction data should be collected. This yields ca. 20 000 reflections up to $\theta = 25°$ where each reflection should be scanned for 3 to 5 min to obtain the required accuracy. With a conventional diffractometer such a measurement would require about two months. In contrast, essentially the same experiment using a CCD-type area detector can be conducted within one day.

Because the oxygen positions of the H_2O molecules in armenite and milarite are very similar (Armbruster et al. 1989; Armbruster and Czank 1992) and the H_2O arrangement is believed to be one of the sources of anomalous optical properties in milarite, the other aim of this study is a comparison of H_2O orientations in armenite and milarite applying single-crystal FTIR spectroscopy. It is expected that the different Si/Al ratio in the framework of armenite and milarite leads also to different orientations of the H-H vectors of H_2O molecules in both minerals, although the position of the H_2O oxygen site is very similar.

Experimental methods

Sample selection

The previous study of armenite (Armbruster and Czank 1992) left open questions about Si, Al ordering and H_2O arrangement in armenite from Rémigny, Quebec, Canada (Pouliot et al. 1984) and from Wasenalp, Valais, Switzerland (Senn 1990). Both samples have a constant Si/Al ratio of 9/6 but different superstructures. An additional reason for selecting these two samples is the availability of sufficient material for MAS NMR spectroscopy.

The milarites studied for comparison were selected because crystal structure refinements and chemical analyses were already published for these samples (Černý et al. 1980; Armbruster et al. 1989) and because material of sufficient quality and quantity was available. Milarite from Val Giuf, Graubünden, Switzerland, has the composition $K_{1.15}Na_{0.05}Ca_{2.09}Al_{0.63}Be_{2.37}Si_{12}O_{30}\cdot 0.6H_2O$ (Armbruster et al. 1989), and the one from Rössing, Namibia, has the composition $K_{1.10}Na_{0.16}Ca_{2.00}Mn_{0.02}Al_{0.66}Be_{2.34}Si_{12}O_{30}\cdot 0.77H_2O$ (Černý et al. 1980).

^{29}Si MAS NMR

Four samples were studied. (1) a hand-picked concentrate of armenite from Rémigny, Quebec, Canada (Pouliot et al. 1984). Due to the small amount of sample available, the armenite powder was diluted with KBr. (2) A powder of armenite from Wasenalp, Valais, Switzerland, was ground from a crystal fragment about 1 cm in diameter (provided by Andres Martin). (3) Three transparent single-crystals of milarite from Val Giuf, Switzerland, were crushed to a powder. (4) A powder was prepared from one greenish translucent crystal of milarite from Rössing, Namibia. All samples were checked by Guinier X-ray photographs prior to NMR to ensure that no other silicate phases were admixed.

The milarite spectra were measured in their natural state and after dehydration 24 h at 800 °C. All NMR spectra were recorded at room temperature at 59.6 MHz (spinning rate 2770 Hz) on a Bruker MSL300 NMR spectrometer (courtesy of A. Sebald and L. Merwin, Bayreuth, Germany). Recycle delays were varied between 10 and 60 s. The spectra (Fig. 2) were collected with recycle delays of 30 s and pulse duration of 2.5 μs corresponding to a 40° flip angle. Typically between 900 and 2800 transients were accumulated. No line broadening or base line corrections were applied. Isotropic chemical shifts δ (^{29}Si) are given relative to δ (^{29}Si) $Si(CH_3)_4$ = 0 ppm as the external reference; δ (^{29}Si) values are accurate within ±0.1 ppm.

Single-crystal X-ray data collection and refinement

The same crystal from Rémigny (Quebec, Canada) as used by Armbruster and Czank (1992) was reinvestigated in this study. An optically homogeneous crystal disk (0.075 mm thick and 0.200 mm in diameter) was separated from a thin section by the microscopic milling technique (Medenbach 1986) and mounted on a three-circle Siemens SMART system equipped with a CCD area detector. Details of the data collection are summarized in Table 1. Data reduction including Lorentz and polarization corrections were performed with the program SAINT (Siemens 1996). An empirical absorption correction based on ψ-scans was applied, which reduced the internal R value from 5.12 to 3.96%. The structure was solved and refined (program SHELXL93 by Sheldrick 1993) in space group *Pnc*2 leading to pronounced correlations (<89%) between atoms related by a pseudo-center of symmetry. Nevertheless, the refinements converged with individual isotropic displacement parameters for all T and O sites. A centrosymmetric refinement (space group *Pnna*) of data collected on the same crystal with a conventional X-ray detector has been reported by Armbruster and Czank (1992). This model yielded substantial Si, Al disorder.

Based on T-O distances Si and Al scattering curves were assigned. Highest peaks in the final difference Fourier maps were 1.45 and −1.2 e/Å^3. Positive peaks are between Ca and coordinating O. The absolute structure could be determined without any indication of twinning by the pseudo-center of symmetry. This is confirmed by the low absolute structure parameter x = 0.07(2) (Flack 1983). Tetrahedral T_c and T_d sites, and O1, O2, and O3 were labeled as described above where the additionally affixed characters are arbitrary tags for identification. An Al or Si at the end of the T label indicates whether the tetrahedron is occupied by Al or Si. W1 and W2 are the O positions of the H_2O molecules.

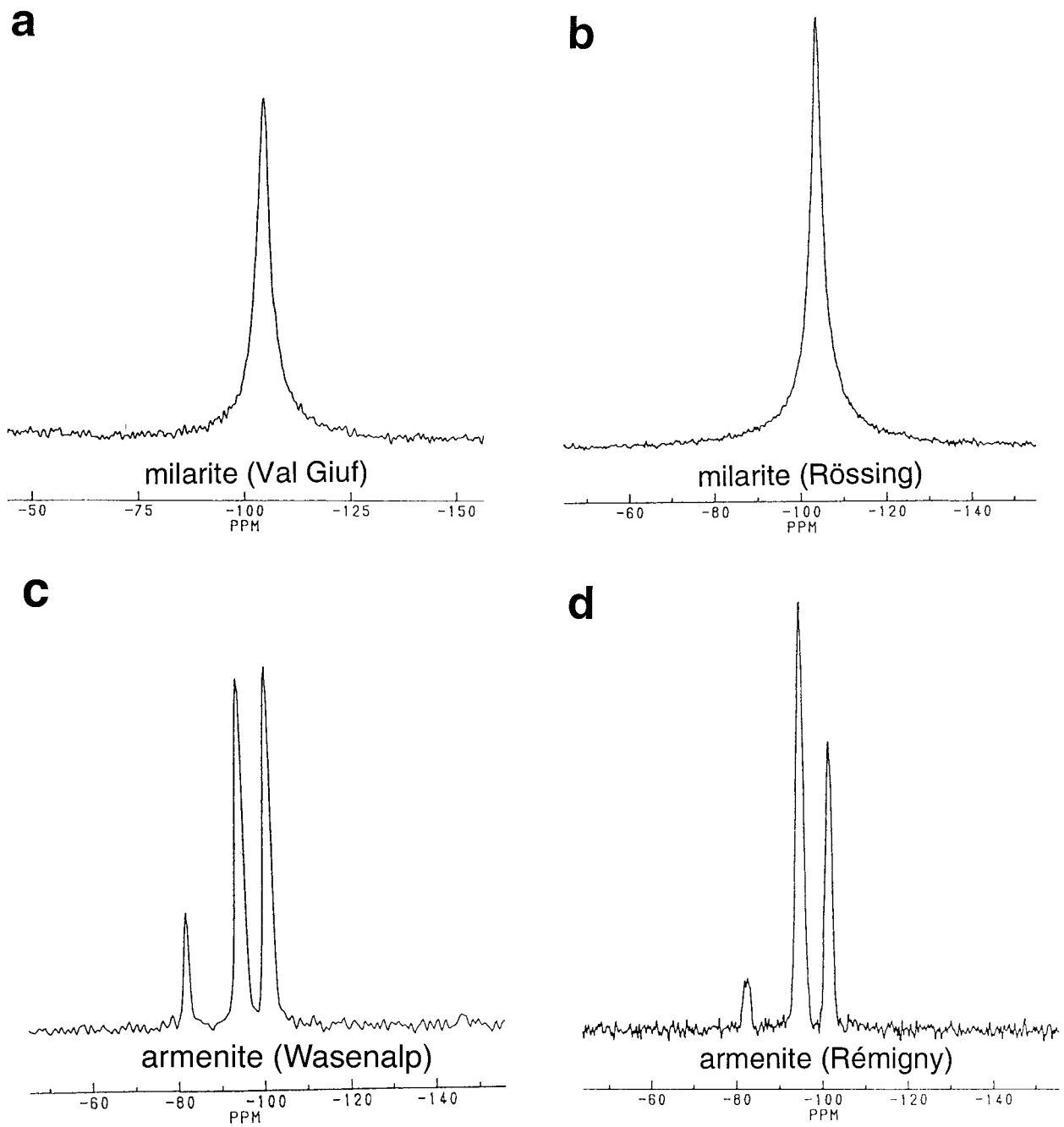

FIGURE 2. ^{29}Si MAS NMR spectra of double-ring silicates. (**a**) Milarite from Val Giuf (Switzerland); (**b**) milarite from Rössing (Namibia); (**c**) armenite from Wasenalp (Switzerland); (**d**) armenite from Rémigny (Canada).

Single-crystal FTIR spectroscopy

Thin, doubly polished slabs were used for IR spectroscopy. Armenite from Wasenalp, Valais, Switzerland, was available in large (centimeter sized) pseudo-hexagonal prismatic crystals. Sections perpendicular to the pseudo-hexagonal *c* axis showed sectors and lamellae with strongly undulatory extinction under the polarizing microscope (crossed polarizers). One section perpendicular to the pseudo-hexagonal *c* axis was 0.038 mm thick, whearas another section parallel to the pseudo-hexagonal *c* axis was 0.050 mm thick. Milarite from Val Giuf, Switzerland was prepared as a 0.122 mm thick slab parallel to [001]. All spectra were recorded on a PERKIN ELMER 1760X FT-IR spectrometer (courtesy of A. Beran and E. Libowitzky, Universität Wien, Austria). The measuring spot was limited to 1 mm by a field aperture. In-

TABLE 1. CCD data collection and refinement of armenite

Diffractometer	Siemens SMART CCD system
X-ray radiation	sealed tube graphite monochromated Mo$K\alpha$
X-ray power	50 kV, 40 mA
Temperature	293 K
Detector to sample distance	5.18 cm
Detector 2Θ angle	27°
Resolution	0.77 Å
Rotation axis	ω
Rotation width	0.3°
Total number of frames	2082
Frame size	512 × 512 pixels
Data collection time per frame	60 s
Collection mode	full sphere of the reciprocal space
Reflections measured	22506
Mean $I/\sigma(I)$	14.96
max. 2Θ	54.7; $-23 \le h \le 23$, $-13 \le k \le 13$, $-17 \le l \le 17$
Unique reflections	5647
Reflections $> 2\sigma(I)$	4275
Space group, cell dimensions	*Pnc*2, a = 18.660(2), b = 10.697(1), c = 13.874(2) Å
R_{int}	3.97% after empirical abs. correction
R_σ	2.76%
Number of l.s. parameters	214
GooF	1.168
$R1$, $F_o > 4\sigma(F_o)$	3.60%
$R1$, all data	5.78%
$wR2$ (on F^2)	9.42%
Flack × parameter	0.07(2)

Notes: $R1 = (\Sigma| |F_o| - |F_c| |)/(\Sigma|F_o|)$; $wR2 = \sqrt{[\Sigma(F_o^2 - F_c^2)^2]/[\Sigma w(F_o^2)^2]}$; GooF = $\sqrt{[\Sigma w(F_o^2 - F_c^{22})^2]/(n - p)}$.

tensities were collected with a liquid nitrogen cooled MCT detector. Polarized spectra were measured parallel and perpendicular to the pseudo-hexagonal *c*-axis between 5700 and 1300 cm^{-1} at a resolution of 4 cm^{-1}. In addition, the armenite slab, cut perpendicular to the pseudo-hexagonal *c*-axis, was measured at different polarizer orientations. Each of the spectra was averaged from 100 single measurements to minimize the background noise. Due to the sample thickness and high H_2O concentration, some very strong absorptions did not transmit light at band center.

RESULTS

^{29}Si MAS NMR

Both milarites show only one strongly broadened band of Lorentzian peak shape assigned to T_d tetrahedra (Fig. 2, Table 2). For the Val Giuf sample the band is at −104.8 ppm. The milarite from Rössing, Namibia, displays the band at −104.3 ppm. After 24 h heat treatment at 800 °C the band remains broad and is centered at 104.5 ppm. There is no indication of Si on T_c.

Both armenites have ^{29}Si MAS NMR characterized by three bands at about −82.5, −95.0, and −101.6 ppm (Fig. 2, Table 2). However, the relative intensities of these bands differ significantly between these two samples. In the Wasenalp armenite, the bands at −95.0 and −101.6 ppm are approximately of equal size and the −82.5 band has about ¼ intensity of the former two. In the Rémigny armenite the intensity distribution is 6% at −82.5, 59% at −95.0, and 35% at −101.6 ppm. Intensities were estimated by multiplying the peak half-width by the height.

Structure refinement

Atomic coordinates are in Table 3, and selected interatomic distances are summarized in Table 4. The *Pnc*2 structure yielded 12 symmetry independent T_d (all on general positions) and 5 T_c sites (only one on a general position). Mean T-O distances cluster in two groups, one group with T-O distances between 1.615 and 1.629 Å, the other group with T-O distances between 1.734 and 1.742 Å. The tetrahedra with short T-O distances were assigned to Si, those with long T-O distances to Al. The arrangement of Si and Al is in agreement with the Loewenstein's (1954) rule. There are four T_d and three T_c sites filled with Al, thus Si and Al are completely ordered in the investigated armenite crystal. A partially occupied (11%) position labeled CC occurred at the cage center of the

TABLE 2. ^{29}Si chemical shifts (in parts per million) from MAS NMR data of double-ring silicates and related compounds

		Band assignment			
Mineral	Tetrahedron	4Al	3Al1Si	2Al2Si	1Al3Si
armenite*	T_c	−82.3			
	T_d		−95.0	−101.8	
high-cordierite†	T_c	−80.0	−82.9	−86.1	
	T_s	−96.7	−101.3	−106.4	−110.3
low-cordierite‡	T_c	−79.7			
	T_s		−100.7		
cord Be 100†	T_s			−106.2	
	T_s			−103.9 [BeAl2Si]	
	T_s			−101.6 [2Be2Si]	
beryl§	T_s			−102.3	
milarite*	T_d				−104.5 [1(Be,Al)3Si]
roedderite‖	T_d				−100.6 [1Mg3Si]

Notes: T_d: double-ring tetrahedra, T_s: single-ring tetrahedra, T_c: ring-connecting tetrahedra. Specific speciation is shown in square brackets.
* This study.
† Hölscher and Schreyer (1989).
‡ Putnis et al. (1985).
§ Sherriff et al. (1991).
‖ Hartman and Millard (1990).

TABLE 3. Atomic coordinates and B_{eq} values for armenite from Rémigny (Canada) refined in space group *Pnc*2.

atom	x/*a*	y/*b*	z/*c*	B_{eq} (Å^2)
Ba	0.25003(7)	0.75472(3)	0.06890(6)	1.165(6)
Ca1	0.4182(1)	0.2475(2)	0.0516(3)	1.11(1)
Ca2	0.0825(1)	0.2536(2)	0.0931(2)	1.11(1)
T_d1Si	0.2956(1)	0.4581(3)	0.2070(2)	0.36(5)*
T_d2Al	0.1302(2)	−0.0512(3)	−0.2970(2)	0.70(5)*
T_d3Si	0.5830(2)	0.3321(3)	0.2066(2)	0.49(5)*
T_d4Si	0.2081(2)	0.0460(3)	0.2103(3)	0.77(5)*
T_d5Al	0.3722(2)	0.9560(3)	0.2081(2)	0.49(5)*
T_d6Si	0.0857(2)	0.6609(3)	−0.2940(2)	0.54(5)*
T_d7Al	0.5889(2)	0.3328(3)	0.4352(3)	0.62(5)*
T_d8Al	0.0851(2)	0.6725(3)	−0.0662(3)	0.64(5)*
T_d9Si	0.2890(2)	0.4547(3)	0.4313(3)	0.42(5)*
T_dASi	0.1252(2)	0.5325(3)	0.4324(2)	0.61(5)*
T_dBSi	0.3721(1)	0.9602(2)	0.4370(2)	0.44(4)*
T_dCSi	0.2090(2)	0.4597(3)	−0.0622(3)	0.72(5)*
T_c1Al	0.2511(3)	0.2530(1)	0.0719(3)	0.48(2)*
T_c2Al	0	0	0.0659(4)	0.33(7)*
T_c3Si	0	1/2	0.0674(4)	0.34(7)*
T_c4Si	1/2	0	0.0747(4)	0.82(8)*
T_c5Al	1/2	1/2	0.0746(4)	0.78(8)*
O11	0.3851(4)	0.9925(8)	0.3276(4)	1.0(2)*
O12	0.2941(5)	0.4229(9)	0.3191(5)	1.3(2)*
O13	0.1077(4)	−0.0104(7)	−0.1780(4)	1.0(2)*
O14	0.4415(4)	0.6622(8)	0.3188(5)	1.1(2)*
O15	0.2049(5)	0.0820(8)	0.3245(5)	1.1(2)*
O16	0.9397(5)	0.1609(8)	0.3166(5)	1.2(2)*
O21	0.2079(3)	0.4973(5)	0.4604(5)	1.0(1)*
O22	0.1249(4)	0.7918(6)	−0.3221(5)	1.3(1)*
O23	0.1152(3)	0.8234(6)	−0.0376(5)	1.1(1)*
O24	0.3564(3)	0.5622(5)	0.1863(4)	1.1(1)*
O25	0.3380(3)	0.9270(5)	−0.0399(4)	1.0(1)*
O26	0.1464(3)	0.9455(5)	0.1867(4)	1.1(1)*
O27	0.3807(3)	0.7995(5)	0.1792(5)	0.8(1)*
O28	0.2195(3)	0.5204(5)	0.1741(5)	0.8(1)*
O29	0.2907(3)	0.4994(6)	−0.0353(5)	1.2(1)*
O210	0.2831(3)	0.9818(6)	0.1796(5)	1.2(1)*
O211	0.3784(3)	0.6875(6)	−0.0349(5)	1.0(1)*
O212	0.1604(3)	0.5806(5)	−0.0386(4)	0.77(9)*
O31	0.0700(4)	0.4677(7)	0.1324(5)	0.9(1)*
O32	0.0718(3)	0.4439(6)	−0.5030(5)	0.7(1)*
O33	0.1925(4)	0.1708(7)	0.1470(6)	0.7(1)*
O34	−0.0183(4)	0.1294(7)	0.1362(6)	1.2(2)*
O35	0.1876(4)	0.3388(7)	0.0042(6)	0.8(1)*
O36	−0.0113(4)	0.3736(7)	0.0046(6)	1.3(2)*
O37	0.4832(3)	0.8764(6)	0.0086(5)	0.4(1)*
O38	0.4871(3)	0.6373(6)	0.1404(5)	0.2(1)*
O39	0.3119(4)	0.3350(7)	0.1419(6)	0.8(1)*
O310	0.3069(4)	0.3352(7)	0.4989(6)	0.8(1)*
O311	0.4311(3)	0.0444(6)	0.1370(5)	0.9(1)*
O312	0.4258(4)	0.0405(7)	0.5061(5)	0.9(1)*
W1	0.4252(5)	0.2516(7)	0.3738(6)	2.0(2)*
W2	0.0725(5)	0.2635(8)	0.2683(8)	2.8(2)*
CC†	0.255(3)	0.753(7)	−0.195(4)	1.58*

* Atoms refined isotropically. T_c represents ring-connecting tetrahedra; T_d are double-ring tetrahedra.
† The CC site is occupied by 0.11(1) O.

six-membered double-rings that was assigned to H_2O. It locally increases the Ba coordination from 12 to 14. This H_2O site is 3.28(6) Å from two neighboring Ba positions. Completely occupied H_2O sites (W1 and W2) increase the Ca coordination from sixfold to sevenfold. The distribution of W1 and W2 associated with the related structural distortions are responsible for the primitive lattice. The completely ordered Si, Al arrangement in the tetrahedral framework fulfills requirements of a *C*-centered lattice (Fig. 3). Both, Si, Al ordering and H_2O distribution are responsible for deviation from hexagonal symmetry.

Single-crystal FTIR spectroscopy

The absorption bands and approximate intensities with polarizations parallel and perpendicular to the pseudo-hexagonal *c* axis are listed in Table 5 and shown in Figure 4. In general milarite and armenite show much stronger anisotropy of H_2O related absorption bands than armenite. The band assignments were adopted from Hawthorne et al. (1991).

DISCUSSION

^{29}Si NMR MAS spectroscopy

In the crystal structure of milarite (e.g., Armbruster et al. 1989; Hawthorne et al. 1991) each Si tetrahedron is connected to three additional ring SiO_4 tetrahedra (T_d) and, in addition, to one Be or Al tetrahedron (T_c) interconnecting the $Si_{12}O_{30}$ double-rings. Si with neighboring Be amounts to 73–79%, the remaining Si is linked to Al. Thus in the ^{29}Si MAS NMR spectra one should expect one weak peak for T_d (3Si,1Al) and one strong peak for T_d (3Si,1Be). The spectra, however, indicate only one broad band. From this observation we must assume that (3Si,1Al) and (3Si,1Be) lead to very similar chemical shifts thus the two band structure cannot be resolved. For synthetic cordierite of composition $Mg_2(Al_2Be)Si_6O_{18}$, Hölscher and Schreyer (1989) observed three ^{29}Si MAS NMR bands assigned to Si(2Si,2Al), Si(2Si,1Be,1Al), and Si(2Si,2Be) at −106.2 and −103.9, and −101.6, respectively. However, in this Be-substituted cordierite Si is always adjacent to two additional Si and not to three Si tetrahedra as in the double-ring silicate milarite. In beryls of the composition $Al_2(Be_{3-x}Li_x)Si_6O_{18}$ $[Cs,Li,Na,K]_x$ with $x < 0.45$, Sherriff et al. (1991) observed only one ^{29}Si MAS NMR band that broadened with increasing *x*. Beryl has the same tetrahedral topology as cordierite and each Si is adjacent to two T_s SiO_4 tetrahedra plus two T_c $(Be,Li)O_4$ connecting the rings to a tetrahedral framework. The broadening of the milarite ^{29}Si MAS NMR band has probably similar disorder reasons as reported for beryl: (1) the observed band is a mixture between Si(3Si,Be) and Si(3Si,Al); or (2) milarite possesses a disordered and distorted structure because B type interstices are either vacant or occupied by Na, K, Ca, or H_2O and Al, Be are disordered on T_d. According to Sherriff et al. (1991), such disorder may lead to substitutional MAS NMR broadening. The effect of H_2O is not significant because the broadening remained after dehydration. (3) For the milarite from Rössing, paramagnetic elements (<0.15 wt% MnO) were analyzed (Černý et al. 1980), which are probably responsible for the characteristic Lorentzian peak shape of the milarite spectra. A similar line shape is observed for the Val Giuf sample. Thus we may speculate that low concentrations of Fe and/or Mn are also present in this sample, although electron microprobe analyses (Černý et al. 1980; Armbruster et al. 1989) failed to detect significant Fe and/or Mn concentrations. Low concentrations of paramagnetic elements (lower than resolved from routine electron microprobe analyses) are

TABLE 4. Selected interatomic distances (Å) for armenite in space group *Pnc*2

T_d1Si	O12	1.599(8)	T_d2Al	O22	1.717(7)	T_d3Si	O27	1.607(7)
	O24	1.616(6)		O31	1.738(8)		O24	1.623(6)
	O39	1.625(8)		O28	1.746(6)		O14	1.624(8)
	O28	1.632(6)		O13	1.759(7)		O38	1.632(7)
mean		1.618	mean		1.740	mean		1.621
T_d4Si	O26	1.610(6)	T_d5Al	O11	1.721(7)	T_d6Si	O16	1.606(8)
	O210	1.614(7)		O27	1.729(7)		O34	1.621(8)
	O33	1.625(8)		O210	1.733(7)		O22	1.628(7)
	O15	1.632(8)		O311	1.754(7)		O26	1.628(6)
mean		1.620	mean		1.734	mean		1.621
T_d8Al	O16	1.694(8)	T_d9Si	O12	1.597(8)	T_dASi	O13	1.583(7)
	O23	1.755(7)		O25	1.612(6)		O23	1.607(7)
	O212	1.757(6)		O310	1.620(8)		O21	1.635(7)
	O36	1.762(9)		O21	1.631(7)		O32	1.642(7)
mean		1.742	mean		1.615	mean		1.617
T_dBSi	O11	1.575(7)	T_dCSi	O212	1.614(6)			
	O211	1.631(7)		O29	1.625(7)			
	O29	1.626(7)		O15	1.636(8)			
	O312	1.630(7)		O35	1.637(8)			
mean		1.616	mean		1.628			
T_c1Al	O310	1.732(9)	T_c2Al	O34	1.728(8)	T_c3Si	O36	1.622(8)
	O39	1.731(9)		O34	1.728(8)		O36	1.622(8)
	O33	1.747(9)		O32	1.752(7)		O31	1.624(8)
	O35	1.770(9)		O32	1.752(7)		O31	1.624(8)
mean		1.745	mean		1.740	mean		1.623
T_c4Si	O311	1.620(7)	T_c5Al	O312	1.735(8)			
	O311	1.620(7)		O312	1.735(8)			
	O37	1.639(7)		O38	1.745(7)			
	O37	1.639(7)		O38	1.745(7)			
mean		1.629	mean		1.740			
Ba	O22	2.826(7)	Ca1	O37	2.344(7)	Ca2	O33	2.357(8)
	O211	2.887(7)		O312	2.358(8)		O31	2.366(8)
	O25	2.893(6)		O310	2.374(8)		O34	2.380(8)
	O212	2.914(6)		W1	2.471(9)		W2	2.44(1)
	O27	2.918(6)		O38	2.481(7)		O35	2.489(8)
	O210	2.940(7)		O311	2.487(7)		O36	2.496(8)
	O28	2.956(6)		O39	2.527(8)		O32	2.506(7)
	O23	3.008(6)						
	O21	3.150(6)						
	O29	3.182(6)						
	O26	3.252(6)						
	O24	3.292(6)						

sufficient to cause substantial peak broadening (e.g., Kirkpatrick 1988).

The fully ordered structure model of armenite (Figs. 1 and 3) refined in this paper leads to 44.44% T_d (Si,3Al), 44.44% T_d (2Si,2Al), and 11.11% T_c (4Al). It is known that ring connecting tetrahedra (T_c) in cordierite show more positive ^{29}Si MAS NMR chemical shifts than ring tetrahedra (T_s) and can thus be distinguished (e.g., Putnis et al. 1985; Hölscher and Schreyer 1991). The three MAS NMR bands observed for Wasenalp armenite agree in intensity and relative chemical shifts with a fully ordered Si, Al distribution in agreement with Loewenstein's rule. The line at −82.3 is assigned to T_c(4Al), and the lines at −95.0 and at −101.6 to T_d(Si,3Al) and T_d(2Si,2Al), respectively. These T_d lines are shifted to significantly more positive values compared to the T_s lines of cordierite (−101.3 and −106.4) with the same assignment (e.g., Hölscher and Schreyer 1991), whereas the T_c(4Al) line for cordierite is at −79.5. In double-ring silicates, T_d tetrahedra are linked to three additional T_d tetrahedra and one T_c tetrahedron. This leads for armenite to an average T_d-O-T angle of ca. 145°. In cordierite and beryl, T_s tetrahedra have two T_s and two T_c neighbors leading to an average T_s-O-T angle of 151°. Radeglia and Engelhardt (1985) have shown that the average T-O-T angle at the ^{29}Si atom is correlated with the NMR chemical shift, which agrees qualitatively for cordierite and armenite. The T_c(4Al) tetrahedron in Mg cordierite (T_c-O-T_s angle = 132.5°) has, in addition, two edge-sharing MgO_6 octahedra (e.g., Cohen et al. 1977), whereas T_c(4Al) tetrahedra in armenite (average T_c-O-T_d angle = 130°) have two edge-sharing CaO_7 polyhedra. According to the group-electronegativity concept of Janes and Oldfield (1985), the chemical shift of armenite T_c tetrahedra should be more negative than the one of cordierite T_c tetrahedra, which also agrees with the observation (Table 2).

The Rémigny armenite has ^{29}Si MAS NMR bands that agree in their position with those of an ordered structure (e.g.,Wasenalp armenite), however the intensity ratios are significantly different thus either a more complicated Si, Al distribution pattern or a mixture between various Si, Al ordered variants must be assumed. Pouliot et al. (1984) report that optically biaxial armenite from Rémigny is intermixed with uniaxial domains. The uniaxial crystals occur as individuals and as euhedral core within larger twinned crystals. Ferraris et al. (1991) found a hexagonal Si, Al arrangement for armenite from Sardinia where all

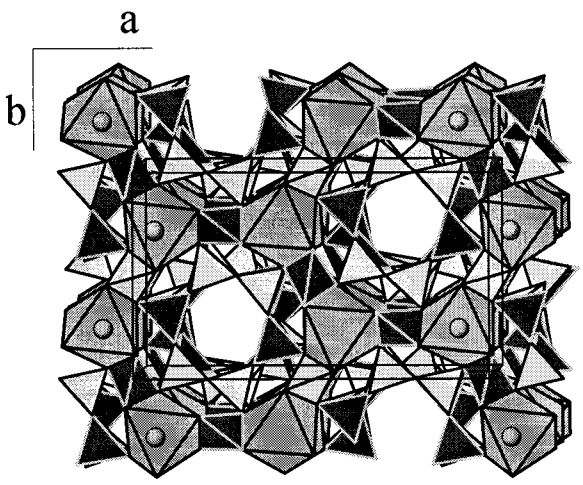

FIGURE 3. Polyhedral representation of the *Pnc*2 armenite structure projected parallel to *c* with unit-cell outlines. Ba is not shown, small spheres are H_2O molecules completing CaO_6 octahedra to sevenfold Ca coordination. Notice the ordered arrangement of H_2O molecules. Where H_2O is not situated above the CaO_6 octahedron it is hidden below the octahedron. Si occupies light tetrahedra with black rims; Al occupies dark tetrahedra with light rims.

T_c tetrahedra are occupied by Al and the twelve T_d tetrahedra are filled with nine Si and three Al in a disordered fashion. Admixture of this armenite modification is in agreement with the decreased intensity of the T_c(4Al) line at −82.3, but various arrangements of the remaining Al in T_d tetrahedra lead inevitably to local T_d(3Si, Al) units for which no lines were observed in the Rémigny spectrum. In addition, the Ferraris et al. (1991) model would yield high concentrations of T_d(2Si,2Al) and only low amounts of T_d(1Si,3Al), contrary to the observed spectrum. If we calculate an average structural formula for the Rémigny armenite on the basis of the T_d, T_c ^{29}Si MAS NMR intensities, we obtain $BaCa_2(Si_{0.54}Al_{2.46})(Si_{8.46}Al_{3.54})O_{30}\cdot 2H_2O$ but we are not able to develop a convincing structural model which is in agreement with a stoichiometric Si/Al ratio of 9/6 (Pouliot et al. 1984), the arrangement of tetrahedra in double-ring silicates, and the observed MAS NMR spectrum.

Structural modifications of armenite

For cordierite two extreme modifications are known, hexagonal high cordierite with random Si, Al distribution in the ring tetrahedra, and *C*-centered orthorhombic low cordierite with a fully ordered Si, Al arrangement. The same holds for armenite. The Si, Al disordered modification (Ferraris et al. 1991), however, is not hexagonal as are milarite (Armbruster et al. 1989), synthetic $BaMg_2Al_6Si_9O_{30}$ (Winter et al. 1995), and high cordierite but orthorhombic (space group *Pnna*), due to the ordered arrangement of H_2O molecules that imposes additional strain on the structure. The Si, Al ordered armenite modification, as exemplified by the present single-crystal X-

TABLE 5. H_2O vibrations in armenite and milarite FTIR data

Peak positions (cm^{-1})	Perpendicular to **c**	Parallel to **c**	Assignment
	Armenite		
5105	weak	weak, broad	$\nu_2\nu_3$
~3620	strong, shoulder	weak, shoulder	ν_3/ν_1
~3420	very strong, broad*	very strong, narrow*	ν_1/ν_3
3250	very weak	weak, narrow	$2\nu_2$
1645	weak, narrow	strong, narrow	ν_2
	Milarite		
5195	weak	—	$\nu_2\nu_3$
~3600	strong, shoulder	weak, shoulder	$\nu_3\nu_1$
~3520	very strong*	strong, narrow	$\nu_1\nu_3$
3220	very weak	weak	$2\nu_2$
1625	medium, narrow	very strong, narrow*	ν_2

* Peaks are off-scale.

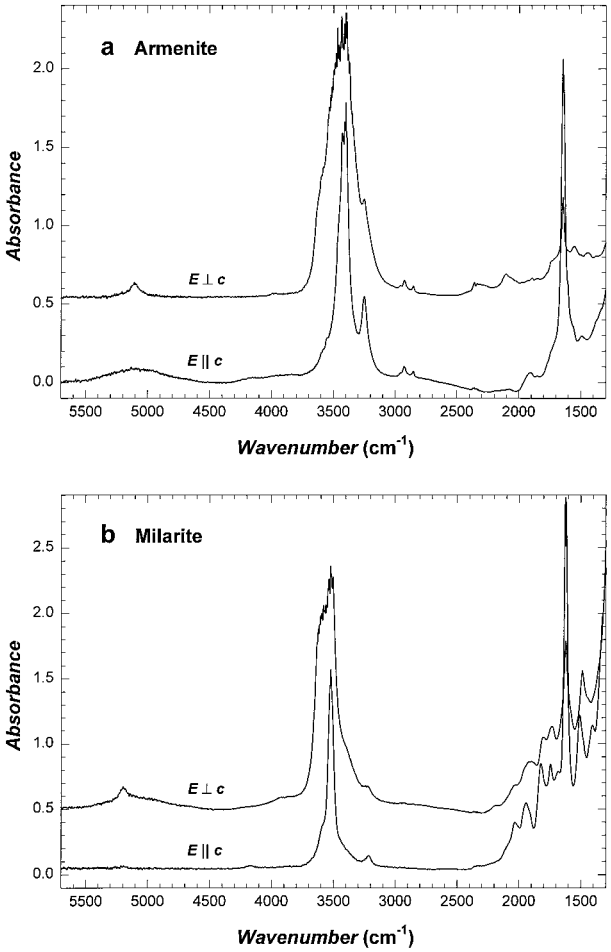

FIGURE 4. Polarized FTIR absorption spectra of (**a**) armenite and (**b**) milarite. For better visibility the $E \perp c$ spectra are vertically offset by 0.5. Due to very strong absorption, bands around 3500 and 1600 cm^{-1} are truncated.

ray data of Rémigny armenite, may adopt *Pnc*2 symmetry. The Si, Al ordering pattern, however, yields a *C*-centered distribution similar to low-cordierite. X-ray reflections with $h + k \neq 2n$ are caused by the arrangement of H_2O molecules and imposed structural distortions. Other ordered H_2O arrangements may lead to different space groups or other translational symmetries as observed for the Wasenalp armenite (Armbruster and Czank 1992). Various H_2O arrangements can be obtained by ordered shifts of the H_2O oxygen site either above or below the center of the B cavity. Thus diffuse reflections of the type $h + k \neq 2n$ are indicative for partial H_2O disorder.

H_2O orientation in milarite

Idealized milarite has the formula $KCa_2(Be_2Al)Si_{12}O_{30}\cdot nH_2O$. However, many natural samples possess an excess of Be and a deficit of Al, which is charge balanced by alkali and alkali earth cations, positioned at the B site (Černý et al. 1980). The B site represents a ninefold-coordinated cavity between two octahedral positions parallel to the *c* axis. Cations on the B site prefer the center of the cavity whereas non-stoichiometric H_2O is displaced parallel to *c* (Armbruster et al. 1989) and has six nearest oxygen neighbors ($3 \times$ O1 and $3 \times$ O3). Calcium octahedra in such an idealized milarite are edge-linked with three T_c tetrahedra, where locally two T_c tetrahedra are occupied by Be and one by Al. This local arrangement reduces the observed $\bar{3}$ average symmetry of Ca. In addition, O3 coordinating Ca is corner linked with a T_d(Si) tetrahedron. Depending on whether O3 links a Be or an Al tetrahedron, the Pauling bond strength of O3 is either one 5/6 (underbonded) or one 13/12 (overbonded). Ow is 2.867 Å from O3 and 2.813 Å from O1 (Armbruster et al. 1989). O1 has an ideal Pauling bond strength of 2.0 because it connects two T_d(Si) tetrahedra. Thus from the view of bond strength, O3 (partially underbonded) is the favorable O to accept a hydrogen bond from Ow. Steric constraints, however, exclude a H_2O proton oriented toward O3 because of short H-Ca distances. The most favorable H_2O proton arrangement is obtained by bifurcated hydrogen bonds to O1 and O3 with H1 (0.319, 0.749, 0.065) and H2 (0.241, 0.579, 0.065). In addition, this proton arrangement is either statically or dynamically disordered governed by the three-fold axis passing through Ow. This model has the H-H vector in (001) and is also in agreement with the polarization of the $\nu_2\nu_3$ combination and the ν_3 asymmetric stretch mode observed in our IR spectra and those of Hawthorne et al. (1991). In the above model the diad of the H_2O molecule is inclined by about 66° to the *c* axis of milarite. A stronger hydrogen bond to O1 decreases the inclination of the H_2O diad. Our IR spectra and those of Hawthorne at al. (1991) show no polarization for the ν_1 mode and incomplete polarization for the ν_2 mode. The polarization of the modes ν_1 and ν_2 determine the orientation of the diad of the H_2O molecule. However, the ν_1, ν_2, ν_3 band assignments of H_2O vibrations suggested by Hawthorne et al. (1991) and adopted in the above model are problematic because ν_1 and ν_2 should show the same polarization (not observed). Thus the assumption of a ''symmetric'' H_2O molecule is questionable. More probable is a H_2O molecule with one ''free'' OH vector leading to the ~3600 cm^{-1} absorption and another with a medium strong hydrogen bond causing the ~3500 cm^{-1} absorption. A more detailed discussion of the exact H_2O orietation is hampered by the fact that milarite crystals show parallel to (001) anomalous optical properties (e.g., sectoring), indicating symmetry lowering. Thus a hexagonal model is not appropriate to derive detailed H_2O orientations.

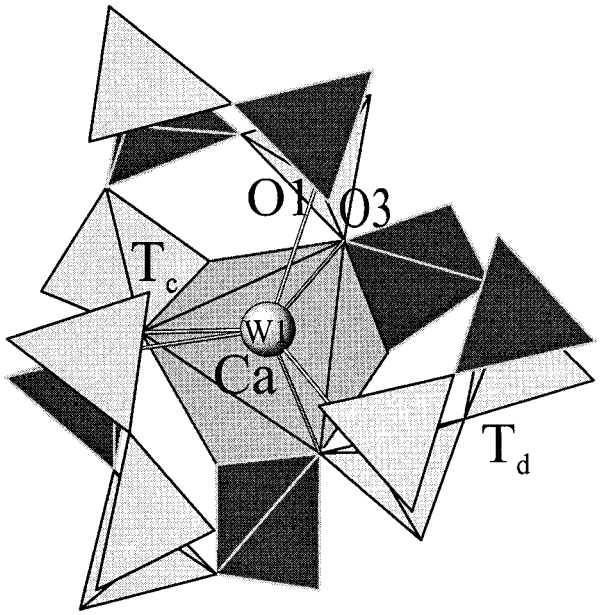

FIGURE 5. Polyhedral represenation of the H_2O environment in armenite. The sphere represents W1 positioned on a pseudo-threefold axis (parallel to *c*); bonds are drawn to the six closest O neighbors ($3 \times$ O3 and $3 \times$ O1). The CaO_6 octahedron below shares O3 type edges with T_c tetrahedra. Four-membered rings of T_d tetrahedra (seen edge-wise) are fragments of the double-ring units. Si occupies light tetrahedra with black rims; Al occupies dark tetrahedra with light rims. The H_2O molecule is slghtly shifted toward the O1-type O atoms connecting an SiO_4 and an AlO_4 T_d tetrahedron.

H_2O orientation in armenite

Figure 5 shows the local environment of W1 in a completely Si, Al ordered armenite, as derived from the ^{29}Si MAS NMR spectra of the Wasenalp sample and the present *Pnc*2 structure refinement. There are three O3 type O atoms (O37, O312, and O310) close to W1 (ca. 2.9 Å apart) and participating in Ca-O bonds. These O3 type O atoms connect an Si tetrahedron and an Al tetrahedron with Ca and are slightly overbonded. W1 is additionally coordinated by three O1 type O atoms (O14, O11, and O12) with O14 and O11 connecting Si and Al tetrahedra whereas O12 links two Si tetrahedra. Thus the slight underbonding of O14 and O11 makes those O atoms pre-

ferred acceptors of weak hydrogen bonds. This is also confirmed by the position of W1, which is 2.759 Å from O14 and 2.941 Å from O11 but 3.149 Å from O12. This would cause the H-H vector to be almost parallel to pseudo-hexagonal (001) which is not supported because the single-crystal IR-spectra show no significant polarization for $\nu_2\nu_3$ and ν_3 modes. The spectra support a H_2O model where one proton is hydrogen bonded to the closest O14 with the second proton rotationally disordered. A similar situation is found around W2 where O16 and O13 have distances of 2.793 Å and 2.821 Å to W2.

References cited

Armbruster, T. and Czank, M. (1992) H_2O ordering and superstructures in armenite $Ca_2Al_6Si_9O_{30}\cdot 2H_2O$: A single-crystal X-ray and TEM study. American Mineralogist, 77, 422–430.

Armbruster, T., Bermanec, V., Wenger, M., and Oberhänsli, R. (1989) Crystal chemistry of double-ring silicates: Structures of natural and dehydrated milarite at 100 K. European Journal of Mineralogy, 1, 353–362.

Armbruster, T., Libowitzky, E., Diamond, L., Auerhammer, M., Bauerhansl, P., Hoffmann, C., Irran, E., Kurka, A., and Rosenstingl, H. (1995) Crystal chemistry and optics of bazzite from Furkabasistunnel (Switzerland). Mineralogy and Petrology, 52, 113–126.

Balassone, G., Boni, M., Di Maio, G., and Franco, E. (1989) Armenite in southwest Sardinia: first recorded occurrence in Italy. Neues Jahrbuch für Mineralogie, Monatshefte, 1989, 49–58.

Černý, P., Hawthorne, F.C., and Jarosewich, E. (1980) Crystal chemistry of milarite. Canadian Mineralogist, 18, 41–57.

Cohen, J.P., Ross, F.K., and Gibbs, G.V. (1977) An X-ray and neutron diffraction study of hydrous low cordierite. American Mineralogist, 62, 67–78.

Ferraris, G., Ivaldi, G., Balassone, G, and Franco, E. (1991) Struttura cristallina di una armenite con simmetria ortorombica. Plinius, 6, 148–149.

Flack, H.D. (1983) On enantiomorph-polarity estimation. Acta Crystallographica, A39, 876–881.

Fortey, N.J., Nancarrow, P.H.A., and Gallagher, M.J. (1991) Armenite from the Middle Dalradian of Scotland. Mineralogical Magazine, 55, 135–138.

Hartman, J.S. and Millard, R.L. (1990) Gel synthesis of magnesium silicates: A ^{29}Si Magic Angle Spinning NMR study. Physics and Chemistry of Minerals, 17, 1–8.

Hawthorne, F.C., Kimata, M., Černý, P., Ball, N., Rossman, G., and Grice, J.D. (1991) The crystal chemistry of the milarite-group minerals. American Mineralogist, 76, 1836–1856.

Hölscher, A. and Schreyer, W. (1989) A new synthetic hexagonal BeMg-cordierite, $Mg_2[Al_2BeSi_6O_{18}]$, and its relationship to Mg-cordierite. European Journal of Mineralogy, 1, 21–37.

Janeczek, J. (1986) Chemistry, optics and crystal growth of milarite from Strzegom, Poland. Mineralogical Magazine, 50, 271–277.

Janes, N. and Oldfield, E. (1985) Prediction of Silicon-29 nuclear chemical shifts using a group electronegativity approach: Applications to silicate and aluminosilicate structures. Journal American Chemical Association, 107, 6769–6775.

Kirkpatrick, R.J. (1988) MAS NMR spectroscopy of minerals and glasses. In Mineralogical Society of America Reviews in Mineralogy, 18, 341–403.

Loewenstein, W. (1954) The distribution of aluminum in the tetrahedra of silicates and aluminates. American Mineralogist, 39, 92–96.

Mason, B. (1987) Armenite from Broken Hill, Australia, with comments on calciocelsian anf barium anorthite. Mineralogical Magazine, 51, 317–318.

Medenbach, O. (1986) Ein modifiziertes Kristallbohrgerät nach Verschure (1978) zur Isolierung kleiner Einkristalle aus Dünnschliffen. Fortschritte der Mineralogie, 64, Beiheft1, 113.

Neumann, H. (1941) Armenite, a water-bearing barium-calcium-alumosilicate. Norsk Geologisk Tidsskrift, 21, 19–24.

Pouliot, G., Trudel, Valiquette, G., and Samson, P. (1984) Armenite-thulite-albite veins at Rémigny, Quebec: The second occurrence of armenite. Canadian Mineralogist, 22, 453–464.

Putnis, A., Fyfe, C.A., and Gabbi, G.C. (1985) Al, Si ordering in cordierite using 'magic angle spinning' NMR. I. ^{29}Si spectra of synthetic cordierites. Physics and Chemistry of Minerals, 12, 211–216.

Radeglia, R. and Engelhardt, G. (1985) Correlations of Si-O-T (T = Si or Al) ^{29}Si NMR chemical shifts in silicates and aluminosilicates. Interpretation by semi-empirical quantum-chemical considerations. Chemical Physics Letters, 114, 28–30.

Sheldrick, G.M. (1993) SHELX-93, program for crystal structure determination. University of Göttingen, Germany.

Siemens (1996) SAINT, release 4.0, Siemens Energy and Automation Inc., Madison, WI 53719, USA.

Semenenko, N.P., Litvin, A.L., Sharkin, O.P., Boiko, V.L., Egorova, L.N., Shurdin, G.S., Terets, G.Y., Savitskaya, A.B., and Ilovaiskaya, S.V. (1987) Armenite from northern Dneiper region. Mineralogicheskii Zhurnal, 9, 83–90 (in Russian).

Senegas, J., Grimmer, A.R., Muller, D., Thomas, P., Mercurio, D., and Frit, B. (1991) Determination of the Al/Si distribution in synthetic $K_xMg_2Al_{4+x}Si_{5-x}O_{18}$ ($0 < x \leq 1$) cordierites by ^{29}Si and ^{27}Al MAS-NMR spectroscopy. Journal of Material Sciences, 26, 5053–5059.

Senn, T. (1990) Ba-Gneise and Ba-Kristallisation im Gebiet der Wasenalp VS. Schweizerische Mineralogische und Petrographische Mitteilungen, 70, 167.

Sherriff, B., Grundy, H.D., Hartman, J.S., Hawthorne, F.C., and Černý, P. (1991) The incorporation of alkalis in beryl: Multi-nuclear MAS NMR and crystal structure study. Canadian Mineralogist, 29, 271–285.

Winter, W., Armbruster, T., and Lengauer, C. (1995) Crystal structure refinement of synthetic osumilite-type phases: $BaMg_2Al_6Si_9O_{30}$, $SrMg_2Al_6Si_9O_{30}$ and $Mg_2Al_4Si_{11}O_{30}$. European Journal of Mineralogy, 7, 277–286.

Zak, L. and Obst, P. (1989) Armenite-feldspar veins in basic volcanic rocks from Chvaletice (Czechoslovakia). Casopsis pro Mineralogii a Geologii, 34, 337–351.

Manuscript received May 27, 1998
Manuscript accepted September 10, 1998
Paper handled by Jonathan F. Stebbins